# Stem Cells®

## Regenerative Medicine

# Functional Control of Transplantable Human ESC-Derived Neurons via Optogenetic Targeting

Jason P. Weick,[a] M. Austin Johnson,[a,b,c] Steven P. Skroch,[d] Justin C. Williams,[d] Karl Deisseroth,[e,f] Su-Chun Zhang[a,b,c,g,h,i,j]

[a]Waisman Center, [b]Neuroscience Training Program, [c]Medical Scientist Training Program, [g]Department of Anatomy, and [h]Neurology, [i]School of Medicine and Public Health, [j]WiCell Institute, and [d]Department of Biomedical Engineering, University of Wisconsin-Madison, Madison, Wisconsin, USA, [e]Department of Bioengineering, Stanford University, Stanford, California, USA, [f]Department of Psychiatry and Behavioral Sciences, Stanford School of Medicine, Stanford, California, USA

### Abstract

Current methods to examine and regulate the functional integration and plasticity of human ESC (hESC)-derived neurons are cumbersome and technically challenging. Here, we engineered hESCs and their derivatives to express the light-gated channelrhodopsin-2 (ChR2) protein to overcome these deficiencies. Optogenetic targeting of hESC-derived neurons with ChR2 linked to the mCherry fluorophore allowed reliable cell tracking as well as light-induced spiking at physiological frequencies. Optically induced excitatory and inhibitory postsynaptic currents could be elicited in either ChR2$^+$ or ChR2$^-$ neurons in vitro and in acute brain slices taken from transplanted severe combined immunodeficient (SCID) mice. Furthermore, we created a clonal hESC line that expresses ChR2-mCherry under the control of the *synapsin-1* promoter. On neuronal differentiation, ChR2-mCherry expression was restricted to neurons and was stably expressed for at least 6 months, providing more predictable light-induced currents than transient infections. This pluripotent cell line will allow both in vitro and in vivo analysis of functional development as well as the integration capacity of neuronal populations for cell-replacement strategies. Stem Cells 2010;28:2008–2016

Disclosure of potential conflicts of interest is found at the end of this article.

## Introduction

Human stem cell derived-neurons present both a model system for the study of functional neural development and plasticity [1, 2] as well as a viable source of therapeutically relevant cells for replacement following neurodegeneration [3]. Toward these ends, traditional stimulation and recording techniques have demonstrated many basic physiological capabilities of these neurons including voltage-gated currents, action potential (AP) generation, and synaptic activity [1, 4]. Furthermore, multiple reports have provided evidence that stem cell-derived neurons can receive information from host cells. For example, Brustle and coworkers used cocultures of either mouse (mESC) or human (hESC)-derived neurons with organotypic hippocampal slices. Stimulation of the intact perforant path fibers could elicit postsynaptic responses in the mESC or hESC-derived neurons deposited on the dentate gyrus [2, 5]. Responses in mESC-derived neurons could also be potentiated by paired-pulse facilitation [5]. These findings are further supported by the fact that, in acute slice preparations from transplanted animals, hESC- and induced pluripotent stem cell (iPSC)-derived neurons demonstrated spontaneous excitatory postsynaptic currents (ePSC) [6, 7], which were thought to derive from the host neurons. Thus, current methods have sufficed to establish a postsynaptic role for ESC- and iPSC-derived neurons in neural networks.

However, the inability to specifically stimulate stem cell-derived neurons has proven insufficient to demonstrate graft-to-host connectivity and slowed our understanding of the synaptic plasticity capabilities of these neurons. Attempts to do so have used extracellular stimulation of grafted cells [8–10] or technically challenging dual patch clamp recordings [11]. Although results from these early studies are suggestive of graft-to-host connectivity, the generalized nature of extracellular stimulation and lack of cell identity inevitably leads to questions of specificity [12]. Dual patch clamp methods have failed to show point-to-point synaptic connections, likely due

to low probability of connectivity between two randomly selected neurons [13]. Further, no studies have reported presynaptic or postsynaptic plasticity due to enduring changes in stem cell-derived neurons themselves. Thus, new techniques are needed to accelerate the study of synaptic development, plasticity, and integration of human stem-cell derived neurons.

Channelrhodopsin-2 (ChR2), a light-gated cation channel [14, 15], presents an optical stimulation method that can be genetically targeted (termed "optogenetics") to specific neuronal populations to resolve these issues. Brief (5–15 ms) light pulses applied to ChR2-expressing rodent neurons can reliably induce AP firing at physiological frequencies (up to 50Hz in some cases [12]) while preserving cell viability [16]. Transgenic animals expressing ChR2 in specific neuronal subpopulations have been used to map local and distant neuronal circuits [17, 18], dissect the underlying rhythms of Parkinson's disease [19], and restore function of damaged tissues [20]. Furthermore, although standard physiological techniques have been integral to the characterization of functional adult neurogenesis in rodents [21], the advent of ChR2 technology was necessary to demonstrate that adult stem cell-derived neurons could form functional synaptic connections with adult neurons [22]. Thus, ChR2 presents a unique tool for controlling the physiological output of specific groups of neurons that may now be readily generated from human stem cells.

Here, we have combined optogenetic targeting with directed neural differentiation of hESCs to provide a method to regulate their functional output for basic and translational studies. We used the pan-neuronal *synapsin-1* (*Syn*) promoter [23] to drive ChR2 expression in cells with a variety of neurotransmitter phenotypes. Light stimulation of hESC-derived neurons expressing ChR2 could reliably drive AP frequencies from 5 to 30 Hz, depending on cell maturity. ChR2 stimulation elicited both glutamatergic and GABAergic PSCs both in vitro and within transplanted tissue for at least 6 months. In addition, we created a pluripotent Syn-ChR2-mCherry cell line to circumvent the variable nature of lentiviral transduction and provide a resource for broader investigation into basic and translational studies of hESC-derived neurons.

## MATERIALS AND METHODS

### Creation of Syn-ChR2-mCherry hESC Line and Cell Culture

The *Syn-ChR2-mCherry* transfer vector with humanized codons was created using methods described [24], whereby the CamKII promoter in the *CaMKIIα-hChR2–mCherry* was excised (*PacI, AgeI*) and replaced by the *Synapsin-1* promoter (−422 to +53; kindly donated by Dr. S. Kugler, University of Goettingen, Germany). Lentiviral production and transduction was performed essentially as described [25]. Briefly, 10 μg of *Syn-ChR2-mCherry*, 7.5 μg lentiviral vector pCMVΔ8.7, and 5 μg vesicular stamtitis virus G protein were cotransfected into HEK293FT cells using calcium phosphate. Forty-eight to seventy-two hours after transfection, culture media containing viral particles was collected and filtered through a 0.45-μm filter (Millipore, Billerica, MA, http://www.millipore.com/). Viral particles were concentrated by ultracentrifugation (SW28 rotor, Beckman Coulter, Brea, CA, http://www.beckmancoulter.com/default.asp) at 20,000*g* for 3 hours. Viral pellets were resuspended in the appropriate culture medium and titrated using the Lenti-X qRT-PCR kit (Clontech, Madison, WI, http://www.clontech.com/).

For transduction of hESCs, cells were incubated for 1 hour with ROCK inhibitor [26], followed by treatment with 0.5% Trypsin-EDTA (Invitrogen, Carlsbad, CA, http://www.invitrogen.com/site/us/en/home.html) for 5 minutes and dissociated to single cells in hESC-media [27]. The cell suspension was centrifuged (1,000 rpm for 5minutes) and resuspended with 100 μl of concentrated virus ($10^6$ transducing units/ml) and then incubated at 37°C for 30 minutes. Cells were then plated onto irradiated mouse embryonic fibroblast (MEF) feeder layers and allowed to grow for 10–14 days for colony formation. Individual colonies were expanded and differentiated to determine if lentiviral incorporation of ChR2 construct had occurred. hESCs (WA09 line, P16-40; Syn-ChR2-mCherry, P25-30) were maintained and differentiated as described [1, 27] with the addition of penicillin-streptomycin (100 U–100 μg/ml, Invitrogen) after viral transduction, and B27 supplement (Invitrogen) to differentiated neurons after day 21. Images of neurons derived from the Syn-ChR2-mCherry line were acquired on live cells using an inverted Nikon TE2000S (Nikon Instruments Inc., Melville, NY, http://www.nikon.com/) Microscope with a Photometrics Coolsnap ES CCD camera (Photometrics, Tucson, Az, http://www.photometrics.com/). Comparisons of light-induced ChR2 currents were made between Syn-ChR2 neurons (passage 27–29) and wild-type WA09 hESC-derived neurons (passage 31–33) and consisted of pooled means of 7–9 cell recordings per passage.

### Immunochemical Staining

Immunolabeling of hESC-derived neural progenitor cultures was performed according to previously established methods [27, 28] using polyclonal synapsin-1 primary antibody (1:1,000; Calbiochem, La Jolla, CA, http://www.emdchemicals.com/), an Alexa-Fluor donkey anti-rabbit 488 secondary antibody (1:1,000; Invitrogen) and visualized using a Nikon confocal workstation (D-Eclipse C1, Nikon Instruments Inc.) running EZ-C1 software (v3.5).

### Transplantation

Cell transplantation was performed similar to previously published methods [29]. Briefly, 21- to 35-day-old neuroepithelial aggregates were dissociated with accutase (0.05%; Invitrogen) and resuspended in differentiation media [1, 27] at a concentration of 50,000/μl. Two microliters of cell suspension was injected through microinjection needles with tip diameters of 50–100 μm into the ventricles of 1- to 2-day-old SCID mouse pups that were anesthetized on ice for 3–4 minutes prior to injections.

### Electrophysiology and Data Analysis

Cultured neurons were recorded in a modified Hanks balanced salt solution that contained (in mM): 140 NaCl, 3 KCl, 2 $CaCl_2$, 1 $MgCl_2$, 15 HEPES, and 23 glucose, pH 7.4, 300 mOsm. Application of pharmacological antagonists diluted in extracellular solution was achieved using a gravity-fed drug barrel system. Tetrodotoxin (TTX; 1 μM), bicuculine (BIC; 20 μM), and 6-cyano-7-nitroquinoxaline-2,3-dione (CNQX, 50 μM) were obtained from Sigma (St. Louis, MO, http://www.sigmaaldrich.com/united-states.html). Acute slice preparations were prepared in cutting solution (CS) and artificial cerebrospinal fluid (aCSF) described previously [30]. Coronal slices were prepared from isoflurane-anesthetized mice whereby the frontal cortex was removed and brains were mounted rostral side down on the slicing stage in ice-cold CS. Slices were cut with a sapphire knife (Leica Microsystems, Deerfield, IL, http://www.leica.com/) mounted in a vibrating microtome (VT1000S; Leica Microsystems) also in ice-cold CS. Slices were transferred to a 35°C chamber containing CS for 30 minutes, then, the chamber was allowed to cool to

room temperature. Slices were secured in a custom perfusion chamber with a fine polyethylene mesh (Siskiyou Inc., Grants Pass, OR, http://www.siskiyou.com/) and perfused with aCSF (315 mOsm) continuously bubbled with 95% $O_2$/5% $CO_2$.

All recordings were performed at 21°C–23°C using pipettes with resistances of 3–5 M$\Omega$ that were filled with an intracellular recording solution containing the following (in mM): 121 K-gluconate, 22 KCl, 10 $Na^+$-HEPES, 10 EGTA, pH 7.2, 290 mOsm. Recordings were obtained using a MultiClamp 700B amplifier (Molecular Devices, Sunnyvale, CA, http://www.moleculardevices.com/) and output to a PC running pClamp nine (Molecular devices); signals were filtered at 4 kHz, sampled at 100 kHz using a Digidata 1322A analog-to-digital converter (Molecular Devices). Access resistance was monitored prior to and following recordings, and cells with resistances greater than 25 M$\Omega$ at either point were discarded from analyses. Series resistance was compensated >60% except during PSC recordings where it was not compensated. All data were stored on a computer hard disk and analyzed with clampfit 9.0 (Molecular Devices) or MiniAnalysis (Synaptosoft, Fort Lee, NJ, http://www.synaptosoft.com/) software. The liquid junction potential was post hoc adjusted according to previously published methods ([31]; JPCalc in Clampex; Molecular Devices). For light-induced AP quantitation, current injections were used to maintain resting membrane potential (RMP) at approximately −60mV. PSC analysis was performed using mini analysis software (Synaptosoft). Statistical analysis was performed using one-way ANOVAs and Fisher's least significant difference post hoc tests. Data from the Syn-ChR2-mCherry cell line (Fig. 5C) represents three replicates of at least eight cells per trial.

## ChR2 Stimulation

Light stimulation was achieved by a custom light emitting diode (LED) device using a 1-Watt blue fiber optic LED (470 nm; Cree Lighting Inc., Morrisville, NC, http://www.creeledlighting.com/) coupled to a fiber optic cable. The end of the fiber optic cable was placed 2–5 mm from ChR2-expressing neurons in the recording chamber. Power to the LED was provided by a TIP110 transistor (National Semiconductor, Santa Clara, CA, http://www.national.com). Light intensity was modulated by a potentiometer, and ranged from 0.1 to 1 mW/$mm^2$, with the most stimulations using 0.4 mW/$mm^2$. National Instruments USB-6501 DAQ provided the trigger pulses, with timing controlled by custom LabView software (National Instruments, Austin, TX, http://www.ni.com/labview/).

## RESULTS

### Developmental Dependence of ChR2-Induced APs in Human Neurons

To examine the utility of ChR2 across multiple neuronal populations, we created a lentiviral vector with the ChR2 gene tethered to the mCherry fluorophore controlled by the pan-neuronal *synapsin-1* promoter (Fig. 1A). To verify the specificity of this construct, hESCs were differentiated to neural progenitors, infected with lentiviruses carrying the Syn-ChR2-mCherry cassette at day 21, and allowed to mature for 1 week. At day 28, cells displayed robust mCherry expression that was only observed in postmitotic neurons (PMNs) that also expressed synapsin-1 but not in proliferating neuroepithelial cells (Fig. 1B; [1, 32]).

We have previously demonstrated that hESC-derived neurons progressively mature over an extended time course com-

pared with rodent neurons. This ability is correlated with relatively hyperpolarized RMPs and increased expression of sodium ($Na^+$) and potassium ($K^+$) currents compared with younger cells [1]. Thus, to determine the functional characteristics of ChR2 in hESC-derived neurons, we recorded 10-week-old mCherry$^+$ cells (Fig. 1C) during exposure to 470-nm light (0.4 mW/$mm^2$). At a holding potential of −70 mV, a 500-ms light stimulus elicited inward currents with two components: a larger current with fast decay kinetics, and a smaller-amplitude sustained current (Fig. 1D, i), consistent with previous findings in rodent neurons [16]. In current-clamp, light stimuli elicited similar potentials (Fig. 1D, ii), and most cells (10/11) displayed a clear threshold deflection indicative of AP generation (Fig. 1E, left trace, arrow). Treatment of cells with 1 $\mu$M TTX eliminated the majority of the fast component of the depolarization, suggesting a true ChR2-induced AP (Fig. 1E, right trace). Recordings from mCherry$^-$ cells revealed no light-induced currents, and stimulation of mCherry$^+$ cells with 650-nm light also had no effect (not shown), indicating the specificity of ChR2-induced currents.

To test the ability of ChR2 to trigger trains of APs in hESC-derived neurons, cells were recorded in current-clamp mode at 10 weeks of differentiation but were now presented with brief (5–10 ms) light pulses [16]. At this time point, light stimuli triggered individual APs with high reliability up to 10 Hz, but the fidelity of light-induced APs dropped precipitously at frequencies greater than 10 Hz (Fig. 1F, 1H). However, after 25 weeks of differentiation, cells could routinely fire 20 Hz trains of ChR2-induced APs (Fig. 1G, 1H), with a subpopulation (2/11) that could fire reliably at 30 Hz and nearly at 50 Hz (Supporting Information Fig. 1). Thus, the probability of light-induced AP generation was significantly increased in older cultures at frequencies of 20–40Hz (Fig. 1H; 20 Hz: $p = .03$; 30 Hz: $p = .006$; 40 Hz: $p = .04$, $n = 7$–14 cells per group). Finally, the number of extraneous APs generated during light pulses was extremely small (Fig. 1I), with cells averaging less than one extra AP during light pulse trains at all frequencies tested. Together, these data suggest that Syn-ChR2-mCherry is specifically expressed in human PMNs and can induce rapid physiological responses on millisecond timescales with high fidelity and low "noise."

### Light-Induced PSCs in ChR2$^-$ Cells In Vitro and in Ex Vivo Slice Preparations

Using our differentiation protocol, we have previously demonstrated that without the addition of exogenous morphogens hESCs preferentially adopt a uniformly forebrain fate [28]. These cultures are composed of both glutamatergic and GABAergic neurons, exhibited by the presence of spontaneous ePSCs and iPSCs ([1]). In voltage-clamp mode, we observed that cells expressing ChR2 routinely displayed increases in PSC incidence during and following trains of light-induced escape action currents (Supporting Information Fig. 2, Fig. 2A, i, arrows). PSCs could also be seen when light stimuli failed to initiate escape action currents, suggesting that other ChR2$^+$ cells in close proximity to the recorded cell initiated synaptic currents (Fig. 2A, ii). Alternatively, these PSCs could have arisen from autaptic currents from the recorded cell, although this remains untested. All PSCs recorded could be blocked by a combination of the $\alpha$-amino-3-hydroxyl-5-methyl-4-isoxazole-propionate (AMPA) and $\gamma$-aminobutyric acid (GABA) receptor antagonists CNQX (50 $\mu$M) and bicuculine (BIC) (20 $\mu$M), regardless of the presence of an escaped action current (Fig. 2A, iii–iv), which were verified by treatment with TTX (Fig. 2A, iv). Furthermore, we were able to detect light-induced PSCs in subpopulations
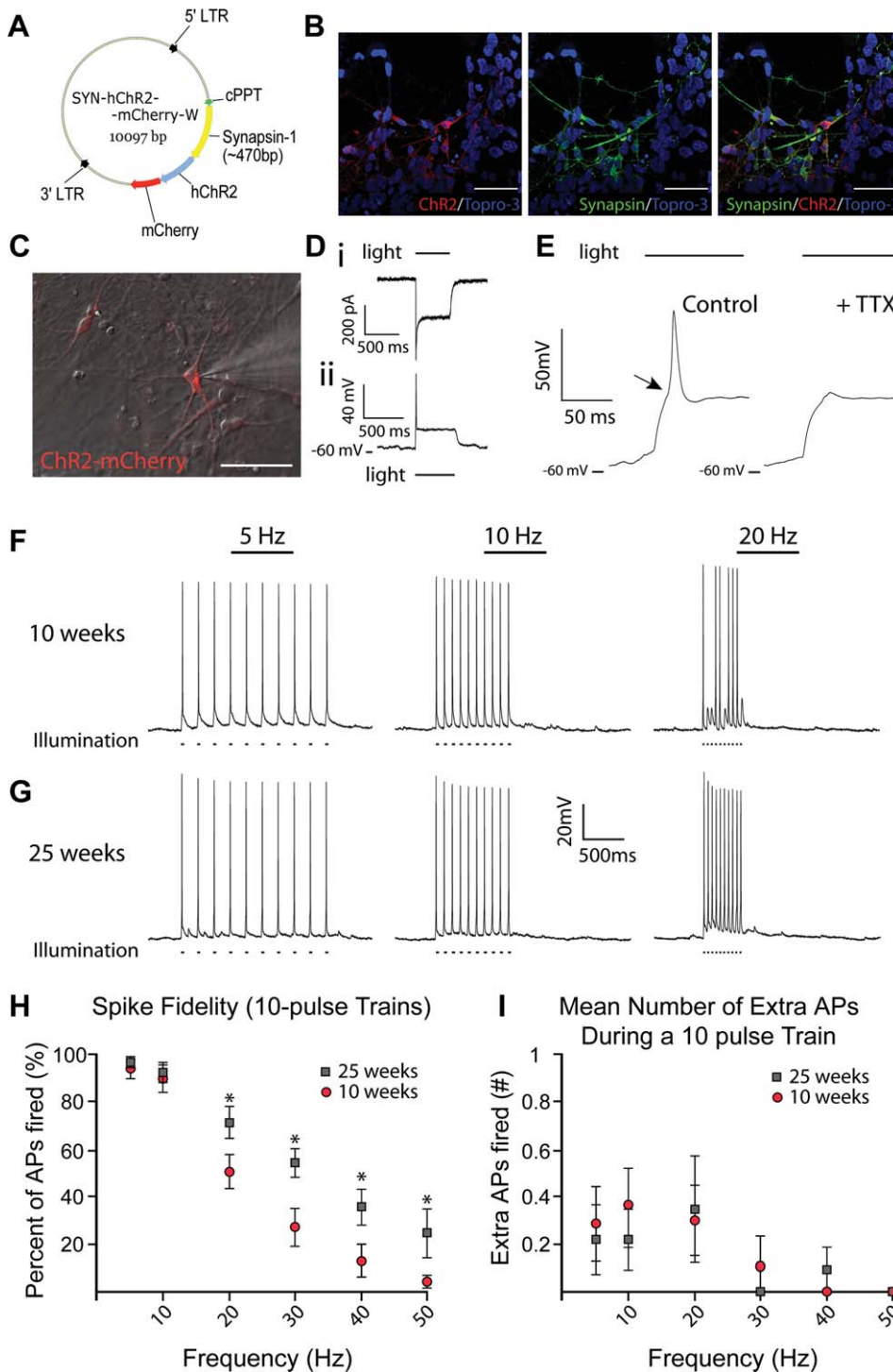
**Figure 1.** Fidelity of ChR2-induced spiking depends on developmental age in human ESC-derived neurons. **(A):** Diagram of lentiviral targeting vector with ChR2 driven by the *synapsin-1* promoter and linked to the mCherry fluorophore. **(B):** Confocal z-stacks of cells expressing *ChR2-mCherry* colocalized with synapsin-1 protein but not in synapsin-1⁻ cells. **(C):** Merged DIC and fluorescent image of a recorded ChR2-mCherry⁺ cell. **(D):** Representative traces from voltage-clamp (i) and current-clamp (ii) recordings of ChR2⁺ cell during a 500 ms, 470-nm light stimulus. **(E):** Expanded timescale of current-clamp recording that demonstrates the presence of an AP by a clear threshold deflection (arrow) and the ability to inhibit the AP by 1 $\mu$M Tetrodotoxin (right trace). **(F, G):** Representative current-clamp traces recorded during 470-nm light stimulations of 5, 10, and 20 Hz for cells differentiated for 10 weeks **(F)** and 25 weeks **(G)**. **(H):** Pooled data demonstrate significant increases in the fidelity of optically induced AP generation in 25-week-old neurons at frequencies of 20–50 Hz. See also Supporting Information Figure 1. **(I):** Chart depicting the mean number of extra spikes fired during 10-pulse trains. *, $p < .05$. Error bars indicate SEM. Scale bars = 50 $\mu$m. Abbreviations: AP, action potential; cPPT, central polypurine tract; ChR2, channelrhodopsin-2; LTR, long terminal repeat; TTX, Tetrodotoxin.

of ChR2⁻ cells (Fig. 2B). A small minority ($n = 2$ of 36) reliably induced ePSCs that were specifically blocked by CNQX (Fig. 2C, i), whereas a larger proportion ($n = 8$ of 36) reliably induced iPSCs that could be blocked by BIC (Fig. 2C, ii). Thus, both glutamatergic and GABAergic populations of cells that expressed ChR2 and could be induced to release neurotransmitter in response to light stimulation.

In addition to pharmacological blockade, we were able to verify that these were truly PSCs (and not ChR2 currents themselves) by their temporal kinetics as well as the delay between stimulus and current onset. In response to 10-ms light stimulations, PSCs had rapid rise times (Fig. 2D, mean = 3.03 ± 0.49 ms, baseline to peak, $n = 8$) as well as a significant delay between light onset and PSC onset (Fig. 2D; mean delay = 21.9 ± 4.2 ms; median delay = 16.3 ms, $n = 10$). In contrast, onset delay for ChR2 currents were uniformly rapid, similar to previous findings (~50 $\mu$s; [33]) and ChR2 current rise times were significantly slower (mean = 10.61 ± 0.39 ms, $n = 10$), making them clearly distinguishable from light-induced PSCs (Supporting Information
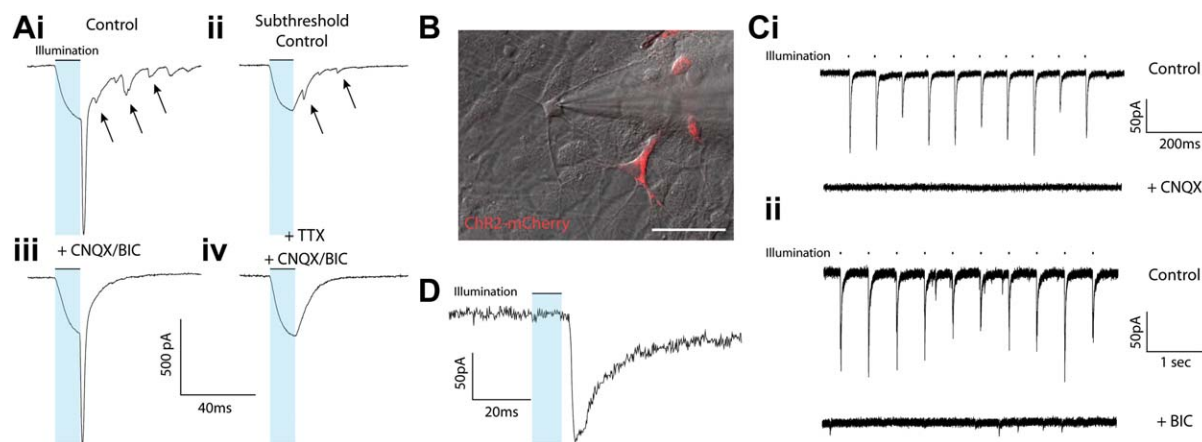
**Figure 2.** Channelrhodopsin-2 (ChR2)-induced postsynaptic currents (PSCs) in human ESC-derived neurons in vitro. **(A):** Voltage-clamp recording of a ChR2$^+$ cell illustrates the presence of PSCs following escape action current (AC) generation (upper left trace) and in response to ChR2 stimulation alone (upper right trace). See also Supporting Information Figure 2A. PSCs recorded after an escape AC or in the absence of an AC could be blocked by a combination of AMPA and GABA receptor antagonists CNQX and bicuculine, respectively (lower traces). **(B):** Combined DIC/fluorescent image of a ChR2$^-$ cell recorded adjacent to ChR2$^+$ cells. **(C):** Excitatory (i, upper trace) and inhibitory (ii, upper trace) PSCs could be generated in two different ChR2$^-$ cells, which were blocked by CNQX (i, lower trace) or BIC (ii, lower trace), respectively. **(D):** Expanded timescale of an individual PSC to illustrate the temporal delay between light stimulus (blue bar) and PSC onset. See also Supporting Information Figure 2B. Scale bar = 50 $\mu$m. Abbreviations: AMPA, α-amino-3-hydroxyl-5-methyl-4-isoxazole-propionate; BIC, bicuculine; CNQX, 6-cyano-7-nitroquinoxaline-2,3-dione; GABA, γ-aminobutyric acid; TTX, Tetrodotoxin.
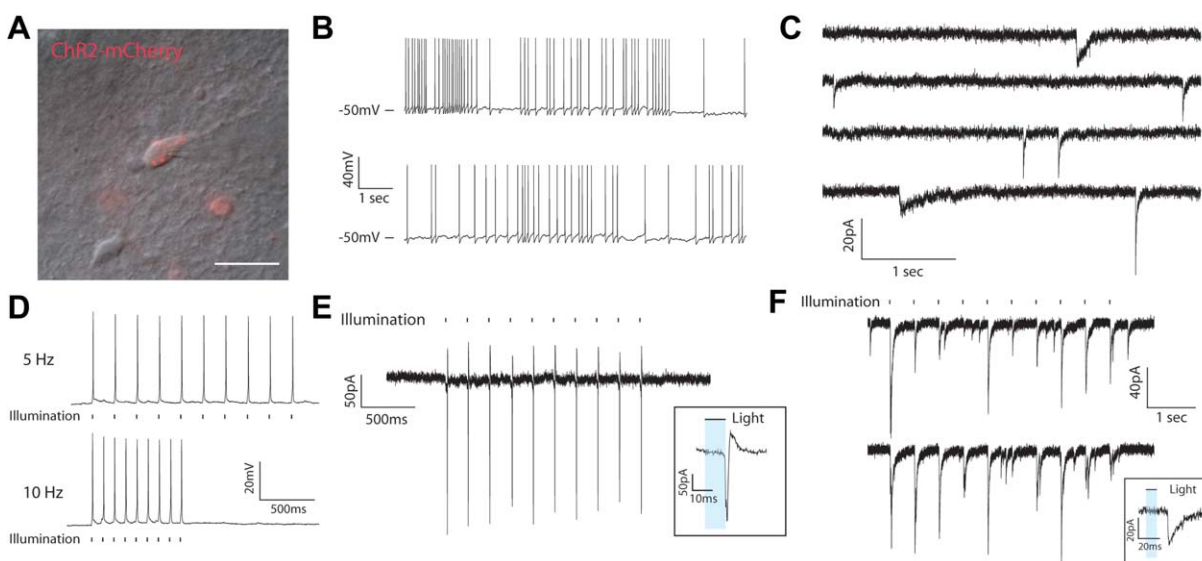


**Figure 3.** Channelrhodopsin-2 (ChR2)-induced currents in human ESC (hESC)-derived neurons in acute slice preparations. **(A):** DIC/fluorescent image of a hESC-derived neuron recorded in an acute slice preparation from a 5-month-old SCID mouse. **(B):** Current-clamp traces demonstrating the presence of spontaneous action potential (AP) generation. **(C):** Voltage-clamp recordings demonstrating the presence of spontaneous postsynaptic currents (PSCs) with different temporal kinetics, indicative of both excitatory and inhibitory synapses. **(D):** Representative current-clamp traces of ChR2-induced spiking at 5 Hz (upper) and 10 Hz (lower) frequencies in response to 470-nm light stimulation. **(E):** Five-hertz train of APs generated in response to light stimulus and recorded in the on-cell configuration, demonstrating the ability of hESC-derived neurons to generate mature spikes (inset) without experimental alteration of resting membrane potential. **(F):** Representative traces from ChR2$^-$ cells that showed PSCs in response to light stimulation of the slice. Inset illustrates the temporal delay between light stimulus (blue bar) and PSC onset. Scale bar = 20 $\mu$m.

Fig. 2). Interestingly, PSC onset delay varied noticeably, ranging from 11.2 to 46.8 ms, likely resulting from a number of factors including across-neuron AP "jitter" (defined as the standard deviation of spike latency). Jitter between hESC-derived neurons (6.3 ± 1.7 ms, $n = 14$) was noticeably greater than what was observed in hippocampal neurons (∼3.4 ms; [16]). However, mean spike latency (16.9 ± 1.7 ms, $n = 14$) and within-cell jitter (2.8 ± 0.5 ms, $n = 14$) did not appear to be different from previous reports. Thus,

increased jitter between hESC-derived neurons likely results from the heterogeneity of the population (e.g., glutamatergic and gabaergic). Importantly, it should be noted that within individual cells, mean PSC onset delay was extremely uniform (0.94 ± 0.18 ms, $n = 10$), suggesting that synaptic transmission at individual synapses was temporally consistent.

To demonstrate the utility of ChR2 expression in hESC-derived neurons within the context of host circuitry, we
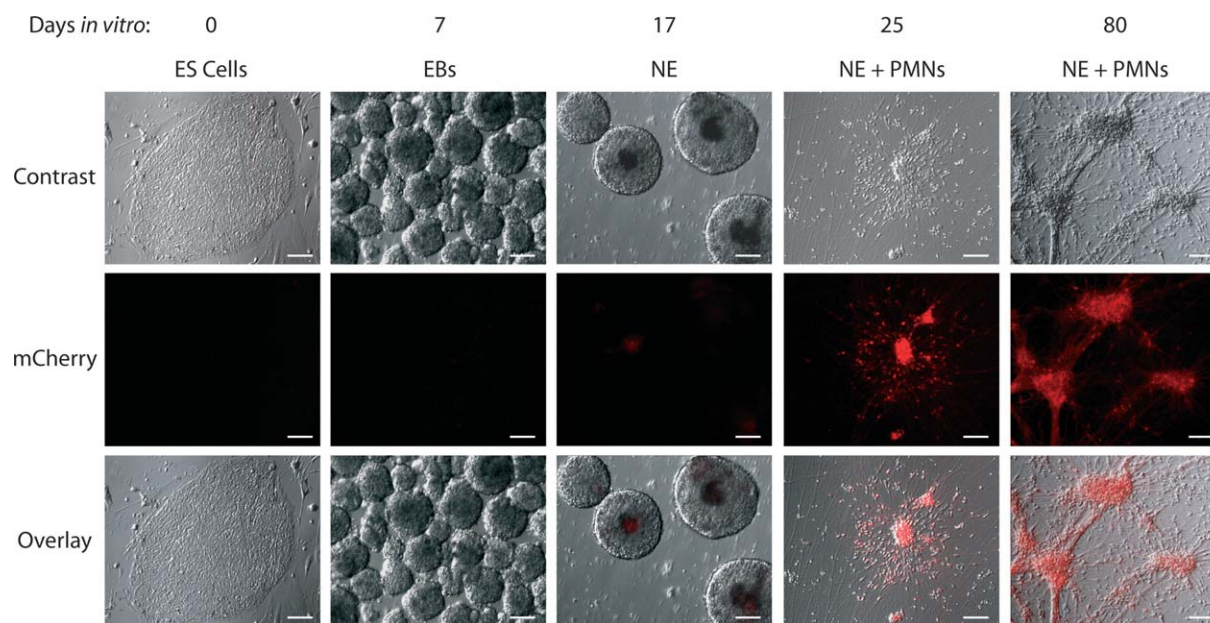
**Figure 4.** A clonal Synapsin-channelrhodopsin-2 (ChR2)-mCherry cell line expresses mCherry on neuronal differentiation. Paired Hoffman contrast and epifluorescent images of differentiating Syn-ChR2-mCherry cells illustrate a lack of ChR2-mCherry expression as ES cells (day 0) and during the embryoid body stage (EBs, days 1–7). Cells remain largely devoid of expression as floating NE (days 7–21) but displayed robust mCherry expression in PMNs at 25 days (column four panels) and 80 days in vitro (column five panels). Scale bars = 100 $\mu$m. Abbreviations: EBs, embryoid bodies; NE, neuroepithelial cell; PMNs, postmitotic neurons.

recorded individual neurons in acute slice preparations 3–6 months after transplantation into perinatal SCID mice (Fig. 3A). hESC-derived neurons at these time points displayed mature physiological phenotypes including low RMPs (mean = −60.7 ± 2.9 mV, $n$ = 19), robust $Na^+$ (137.2 ± 12.2 pA/pF, $n$ = 20), and $K^+$ currents (66.2 ± 7.6 pA/pF, $n$ = 20). Furthermore, hESC-derived neurons displayed spontaneous APs and PSCs, indicating the formation of functional neural networks within host brains (Fig. 3B, 3C). Furthermore, similar to in vitro cultures, APs could be readily induced in mCherry$^+$ neurons by 470-nm light at physiological frequencies (Fig. 3D). Light-induced APs could also be elicited in the on-cell configuration without manipulation of the RMP (Fig. 3E), indicating that the endogenous RMP of these cells was sufficient to allow rapid repolarization following light stimulation. Furthermore, light-induced PSCs could be reliably induced in ChR2$^-$ cells adjacent to ChR2$^+$ neurons (Fig. 3F; light intensity: 1 mW/mm$^2$).

Although ChR2$^-$ neurons were not verified as mouse or human, the data are proof of concept that this is a useful tool to examine the synaptic integration properties of transplanted hESC-derived neurons. Importantly, we can be confident that light-induced currents derived solely from human cells due to a lack of expression observed in anatomically identifiable mouse neurons (e.g., hippocampal formation), and the fact that previous reports found no transfer of heterologously expressed opsins between synaptically connected neuronal populations [34]. It should be noted that for slice recordings, we observed greater failure rates at light intensities <1 mW/mm$^2$ (not shown) and larger variation in PSC amplitude was observed at light intensities of 1 mW/mm$^2$ (Fig. 3F), which was likely due to diffraction of light within the slice [35]. Finally, no exogenous retinal was given to SCID mice following transplantation, indicating that endogenous levels were sufficient to reveal ChR2 currents in acute slice preparations.

## A Pluripotent Syn-ChR2-mCherry hESC Line

Although viral infection of hESC-derived neurons successfully demonstrated the utility of ChR2 in transplantable human neurons, there is inherent variability in transduction efficiency and expression using this method. Thus, we sought to create a clonal hESC line that would express ChR2 following differentiation to synapsin$^+$ neurons. Infection of hESCs followed by trypsinization in the presence of the ROCK inhibitor [26] allowed us to select clones transduced with the Syn-ChR2-mCherry virus. Selection and subsequent differentiation of these cells revealed multiple clones that became mCherry$^+$ during neuronal differentiation. A single clone was chosen based on mCherry fluorescence intensity as well as neuronal differentiation potential without contaminating cell populations. This clone did not display mCherry expression at the hESC stage nor during the early phases of neural induction (Fig. 4; ESCs, embryoid bodies [EBs], neuroepithelial cells [NE]). However, on plating neuroepithelial aggregates after 3 weeks, mCherry expression was observed in the majority of cells with visible neurites (Fig. 4, NE + PMNs, column 4). mCherry expression was maintained in cells for the duration of experiments (Fig. 4, NE + PMNs, column 5), and increased in intensity with many cells becoming visible by eye after 2 months.

To test the functionality of this Syn-ChR2-mCherry cell line, we recorded from neurons between 5 to 6 weeks, 10 to 12 weeks, and 3 to 5 months of differentiation. Although mCherry expression was detectable by 4 weeks (Fig. 4), fluorescence intensity was relatively weak and required detection via CCD camera. Likewise, light stimulation of 5- to 6-week-old cells clamped at a holding potential of −70 mV revealed relatively small ChR2-mediated currents (Fig. 5A, 5B; mean amplitude = 27.6 ± 3.4 pA). Furthermore, stimulation of these cells rarely ($n$ = 1/11) produced AP generation (Fig. 5C, i), likely due to the diminutive nature of the ChR2 current as well as low levels of $Na^+$ and $K^+$ channel expression and
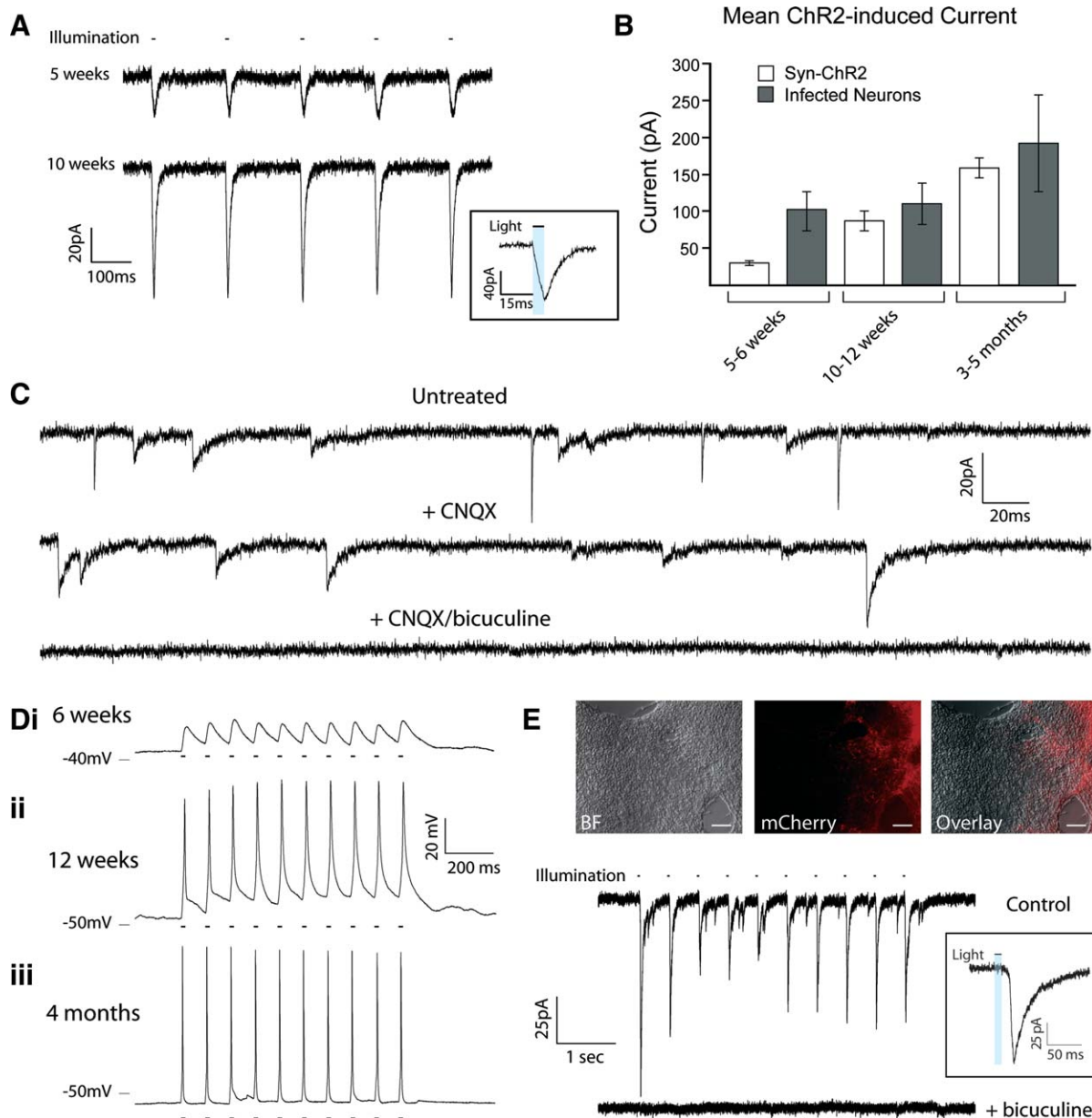
**Figure 5.** Synapsin-channelrhodopsin-2 (ChR2)-mCherry cell line exhibits a full complement of optically induced currents. **(A):** Representative traces of ChR2 currents from Syn-ChR2 neurons at 5 and 10 weeks; inset shows light-current relationship. **(B):** Pooled data demonstrates that the ChR2-mediated currents in the cell line increased during differentiation in response to 10-ms light stimuli and displayed less variation compared with hESC-derived neurons that were infected on differentiation. **(C):** Representative voltage-clamp traces from Syn-ChR2-derived neurons after 10 weeks of differentiation illustrate the presence of excitatory postsynaptic currents (ePSCs) and inhibitory postsynaptic currents (iPSCs). ePSCs were specifically blocked by application of CNQX (50 $\mu$M) and iPSCs were blocked by bicuculine (bicuculine; 20 $\mu$M). **(D):** Representative current-clamp traces from Syn-ChR2-mCherry neurons in response to 10 Hz stimulations at 6 weeks (i), 12 weeks (ii), and 4 months (iii) of differentiation. **(E):** Paired Hoffman contrast and fluorescent images of cocultures of wild-type hESC-derived neurons and Syn-ChR2-mCherry neurons. Representative voltage-clamp recording of a ChR2$^-$ cell that generated postsynaptic currents in response to 470-nm light stimuli (upper trace) and could be blocked with BIC (lower trace). Inset shows light-current relationship. Error bars represent SEM. Scale bar = 100 $\mu$m. Abbreviation: CNQX, 6-cyano-7-nitroquinoxaline-2,3-dione.

RMPs at or above Na$^+$ channel threshold in these immature neurons [1]. However, mean ChR2-induced current amplitude was increased at later time points (10–12 weeks) and were not different from transiently infected cells of similar developmental age (Fig. 5B; $p > .05$, $n = 3$, see Materials and Methods). However, the variability of ChR2-induced currents compared with transient infections at the same time point was significantly decreased (5–6 weeks: $p = .003$; 10–12 weeks: $p = .02$; 3–5 months: $p = .005$; $n = 3$ at each time point) sug-

gesting a greater uniformity of expression in the Syn-ChR2-mCherry cell line. Finally, to establish that our Syn-ChR2 line was capable of generating neurons of multiple transmitter phenotypes that were also fully functional (presynaptically and postsynaptically), we recorded spontaneous PSCs in cultures of Syn-ChR2 cells alone or in coculture with normal WA09 hESC-derived neurons. In Syn-ChR2 cultures, we observed spontaneous PSCs with two distinct temporal profiles indicative of glutamatergic and GABAergic synapses

(Fig. 5C, upper traces), similar to previous studies [1]. Indeed, PSCs with relatively fast kinetics were specifically blocked by CNQX (Fig. 5C, middle traces), whereas those with slower kinetics were blocked by bicuculine (Fig. 5C, lower traces). Although Syn-ChR2 neurons were unable to trigger light-induced APs at 6 weeks, the majority of cells (7/8) at 10–12 weeks could fire at least one AP in response to trains of light stimulation, and some (2/8) could maintain firing rates of up to 10 Hz, although the APs appeared immature in nature (e.g., lack of rapid repolarization, Fig. 5D, ii). At later time points (>3 months), some individual mCherry$^+$ cells became visible to the naked eye, and most (7/10) could fire repetitive trains of APs in response to ChR2 stimulation (Fig. 5D, iii), wherein APs appeared more mature with faster kinetics and reduced refraction times. Finally, in cocultures with wild-type WA09-derived neurons (Fig. 5E, upper panels), recordings from non-ChR2 neurons revealed the presence of repeatable light-induced PSCs that could be blocked with BIC (Fig. 5E, traces), demonstrating their ability to form functional synapses with neurons from other sources.

## DISCUSSION

The present study demonstrates the utility of optogenetic technology for controlling the functional output of transplantable stem cell-derived neurons. In addition to the creation of a pluripotent cell line whose excitability can be optically regulated when differentiated to neurons, our results represent the first demonstration that hESC-derived neurons are fully competent to form functional neural networks in vivo. Previous reports demonstrated that hESC-derived neurons could fire APs and could receive synaptic "input" from host neurons in acute slice preparations [4] or when deposited onto rat hippocampal slice cultures [2, 6]. We have extended these findings to show that hESC-derived neurons transplanted to neonatal SCID mice can act as a functional unit of "output," capable of sending synaptic information to adjacent neurons. The fact that this activity can be regulated by ChR2 activation provides a tool for assessing the activity-dependent nature of synaptic integration and functional recovery following transplantation. This was possible in the absence of exogenous retinol, which is required in some systems [33], indicating that endogenous retinol levels in SCID mouse brains are sufficient for ChR2 activation. Furthermore, survival of ChR2-expressing neurons was maintained for up to 6 months in vivo, raising hopes for longitudinal behavioral studies employing implantable LED or diode laser devices [36].

The combination of hESC and ChR2 technologies has broad potential for basic research as well as applied science. First, hESC/ChR2 technology will simplify the study of functional development and plasticity of human neurons both in vitro and in vivo. For instance, we delineated a temporal dependence of ChR2-mediated AP production in hESC-derived neurons. This technique could be extended to examine synaptic development [37], plasticity [38], or the crosstalk between cation influx (e.g., calcium) and the activation of other receptors such as metabotropic glutamate receptors [39]. ChR2 activation may also facilitate the study of activity-dependent signal transduction and gene expression cascades such as those that occur during neuronal differentiation of stem cells [40]. Finally, it will allow researchers to definitively determine the integration capacity of hESC-derived neurons following transplantation, similar to studies conducted on newly born adult hippocampal neurons [22]. Previous attempts to demonstrate graft-to-host connectivity relied on technically

challenging dual patch clamping methods or nonspecific extracellular stimulations [11]. Now, as we demonstrate in the present study, it is possible to genetically restrict stimulation to the stem cell-derived population while simultaneously amplifying output by activating many transplanted neurons simultaneously. This will increase the probability of demonstrating functional connectivity between various neuronal subclasses, as well as to examine local microcircuitry.

For translational studies, the Syn-ChR2-mCherry hESC line can be combined with directed differentiation of various neuronal subtypes (e.g., midbrain dopamine neurons) and implantable light stimulation devices [36]. This will provide researchers with a minimally invasive tool to examine cell replacement strategies for neurodegenerative disorders in vivo. By modulating the amount of light excitation of ChR2$^+$ neurons one might be able to regulate the therapeutic effects and potentially minimize side effects of transplanted cells. This may be further aided by subsequent genetic modifications that allow for cell-type-specific cell sorting to enhance population purity [41]. Furthermore, ChR2 technology may assist in dissecting the optimal patterns of neural activity (e.g., tonic vs. phasic spiking) necessary for functional recovery of disease models of neurodegeneration such as Huntington's disease, amyotrophic lateral sclerosis, as well as PD. Furthermore, newly developed optrode technologies [42, 43] can be used to detect real time neural excitation during in vivo stimulation as a method to correlate behavioral responses with the degree of hESC-derived neuronal stimulation, similar to in vivo mapping of neural circuitry [19].

Although stem cell-based optogenetic technology represents a significant advancement for regulating the physiological state of transplantable cells, significant challenges still exist for its application. For instance, ChR2 expression level, light intensity, and cellular RMP may all affect the fidelity of light-induced AP firing in individual cells [12, 18]. We have attempted to circumvent one of those issues by creating a cell line with relatively uniform ChR2 expression. Although expression increased with developmental age, the variability of ChR2-induced currents was significantly decreased compared with transient infection at each time point tested and most could respond to light intensities consistent with previous reports in rodent neurons [16, 18]. Thus, a clonal stem cell line offers a source of human neurons with predictable functional responses to light stimulation.

## CONCLUSION

We have used optogenetic targeting to regulate the functional output of neurons derived from hESCs. We characterized a temporal dependence of the light-action potential relationship and demonstrated reliable optically-induced synaptic transmission both in vitro and in ex vivo slice preparations. Furthermore, we have created a pluripotent hESC line that carries the Synapsin-ChR2-mCherry transgene. Neurons derived from this line will be amenable to the examination functional integration and plasticity within the context of a host environment.

## DISCLOSURE OF POTENTIAL CONFLICTS OF INTEREST

The authors indicate no potential conflicts of interest.

## REFERENCES

1 Johnson MA, Weick JP, Pearce RA et al. Functional neural development from human embryonic stem cells: Accelerated synaptic activity via astrocyte coculture. J Neurosci 2007;27:3069–3077.

2 Ladewig J, Koch P, Endl E et al. Lineage selection of functional and cryopreservable human embryonic stem cell-derived neurons. Stem Cells 2008;26:1705–1712.

3 Sonntag KC, Simantov R, Isacson O. Stem cells may reshape the prospect of Parkinson's disease therapy. Brain Res Mol Brain Res 2005;134:34–51.

4 Muotri AR, Nakashima K, Toni N et al. Development of functional human embryonic stem cell-derived neurons in mouse brain. Proc Natl Acad Sci USA 2005;102:18644–18648.

5 Benninger F, Beck H, Wernig M et al. Functional integration of embryonic stem cell-derived neurons in hippocampal slice cultures. J Neurosci 2003;23:7075–7083.

6 Koch P, Opitz T, Steinbeck JA et al. A rosette-type, self-renewing human ES cell-derived neural stem cell with potential for in vitro instruction and synaptic integration. Proc Natl Acad Sci USA 2009; 106:3225–3230.

7 Wernig M, Zhao JP, Pruszak J et al. Neurons derived from reprogrammed fibroblasts functionally integrate into the fetal brain and improve symptoms of rats with Parkinson's disease. Proc Natl Acad Sci USA 2008;105:5856–5861.

8 Bjorklund A, Segal M, Stenevi U. Functional reinnervation of rat hippocampus by locus coeruleus implants. Brain Res 1979;170: 409–426.

9 Low WC, Lewis PR, Bunch ST et al. Function recovery following neural transplantation of embryonic septal nuclei in adult rats with septohippocampal lesions. Nature 1982;300:260–262.

10 Segal M, Bjorklund A, Gage FH. Transplanted septal neurons make viable cholinergic synapses with a host hippocampus. Brain Res 1985; 336:302–307.

11 Kim JH, Auerbach JM, Rodriguez-Gomez JA et al. Dopamine neurons derived from embryonic stem cells function in an animal model of Parkinson's disease. Nature 2002;418:50–56.

12 Zhang F, Wang LP, Boyden ES et al. Channelrhodopsin-2 and optical control of excitable cells. Nat Methods 2006;3:785–792.

13 Debanne D, Boudkkazi S, Campanac E et al. Paired-recordings from synaptically coupled cortical and hippocampal neurons in acute and cultured brain slices. Nat Protoc 2008;3:1559–1568.

14 Nagel G, Szellas T, Huhn W et al. Channelrhodopsin-2, a directly light-gated cation-selective membrane channel. Proc Natl Acad Sci USA 2003;100:13940–13945.

15 Sineshchekov OA, Jung KH, Spudich JL. Two rhodopsins mediate phototaxis to low- and high-intensity light in Chlamydomonas reinhardtii. Proc Natl Acad Sci USA 2002;99:8689–8694.

16 Boyden ES, Zhang F, Bamberg E et al. Millisecond-timescale, genetically targeted optical control of neural activity. Nat Neurosci 2005;8: 1263–1268.

17 Petreanu L, Huber D, Sobczyk A et al. Channelrhodopsin-2-assisted circuit mapping of long-range callosal projections. Nat Neurosci 2007; 10:663–668.

18 Wang H, Peca J, Matsuzaki M et al. High-speed mapping of synaptic connectivity using photostimulation in Channelrhodopsin-2 transgenic mice. Proc Natl Acad Sci USA 2007;104:8143–8148.

19 Gradinaru V, Mogri M, Thompson KR et al. Optical deconstruction of parkinsonian neural circuitry. Science 2009;324:354–359.

20 Bi A, Cui J, Ma YP et al. Ectopic expression of a microbial-type rhodopsin restores visual responses in mice with photoreceptor degeneration. Neuron 2006;50:23–33.

21 Ge S, Goh EL, Sailor KA et al. GABA regulates synaptic integration of newly generated neurons in the adult brain. Nature 2006;439:589–593.

22 Toni N, Laplagne DA, Zhao C et al. Neurons born in the adult dentate gyrus form functional synapses with target cells. Nat Neurosci 2008; 11:901–907.

23 Kugler S, Kilic E, Bahr M. Human synapsin 1 gene promoter confers highly neuron-specific long-term transgene expression from an adenoviral vector in the adult rat brain depending on the transduced area. Gene Ther 2003;10:337–347.

24 Zhang F, Wang LP, Brauner M et al. Multimodal fast optical interrogation of neural circuitry. Nature 2007;446:633–639.

25 Xia X, Zhang SC. Genetic modification of human embryonic stem cells. Biotechnol Genet Eng Rev 2007;24:297–309.

26 Watanabe K, Ueno M, Kamiya D et al. A ROCK inhibitor permits survival of dissociated human embryonic stem cells. Nat Biotechnol 2007;25:681–686.

27 Zhang SC, Wernig M, Duncan ID et al. In vitro differentiation of transplantable neural precursors from human embryonic stem cells. Nat Biotechnol 2001;19:1129–1133.

28 Li XJ, Du ZW, Zarnowska ED et al. Specification of motoneurons from human embryonic stem cells. Nat Biotechnol 2005;23:215–221.

29 Guillaume DJ, Johnson MA, Li XJ et al. Human embryonic stem cell-derived neural precursors develop into neurons and integrate into the host brain. J Neurosci Res 2006;84:1165–1176.

30 Bischofberger J, Engel D, Li L et al. Patch-clamp recording from mossy fiber terminals in hippocampal slices. Nat Protoc 2006;1:2075–2081.

31 Barry PH. JPCalc, a software package for calculating liquid junction potential corrections in patch-clamp, intracellular, epithelial and bilayer measurements and for correcting junction potential measurements. J Neurosci Methods 1994;51:107–116.

32 Weick JP, Johnson MA, Zhang SC. Developmental regulation of human embryonic stem cell-derived neurons by calcium entry via transient receptor potential channels. Stem Cells 2009;27:2906–2916.

33 Nagel G, Brauner M, Liewald JF et al. Light activation of channelrhodopsin-2 in excitable cells of Caenorhabditis elegans triggers rapid behavioral responses. Curr Biol 2005;15:2279–2284.

34 Gradinaru V, Zhang F, Ramakrishnan C et al. Molecular and cellular approaches for diversifying and extending optogenetics. Cell 2010; 141:154–165.

35 Yaroslavsky AN, Schulze PC, Yaroslavsky IV et al. Optical properties of selected native and coagulated human brain tissues in vitro in the visible and near infrared spectral range. Phys Med Biol 2002;47:2059–2073.

36 Aravanis AM, Wang LP, Zhang F et al. An optical neural interface: In vivo control of rodent motor cortex with integrated fiberoptic and optogenetic technology. J Neural Eng 2007;4:S143–S156.

37 Hornstein NJ, Pulver SR, Griffith LC. Channelrhodopsin2 mediated stimulation of synaptic potentials at Drosophila neuromuscular junctions. J Vis Exp 2009;25:pii:1133.

38 Zhang YP, Oertner TG. Optical induction of synaptic plasticity using a light-sensitive channel. Nat Methods 2007;4:139–141.

39 Caldwell JH, Herin GA, Nagel G et al. Increases in intracellular calcium triggered by channelrhodopsin-2 potentiate the response of metabotropic glutamate receptor mGluR7. J Biol Chem 2008;283:24300–24307.

40 Deisseroth K, Singla S, Toda H et al. Excitation-neurogenesis coupling in adult neural stem/progenitor cells. Neuron 2004;42:535–552.

41 Zhou W, Lee YM, Guy VC et al. Embryonic stem cells with GFP knocked into the dopamine transporter yield purified dopamine neurons in vitro and from knock-in mice. Stem Cells 2009;27:2952–2961.

42 Gradinaru V, Thompson KR, Zhang F et al. Targeting and readout strategies for fast optical neural control in vitro and in vivo. J Neurosci 2007;27:14231–14238.

43 Zhang J, Laiwalla F, Kim JA et al. Integrated device for optical stimulation and spatiotemporal electrical recording of neural activity in light-sensitized brain tissue. J Neural Eng 2009;6:55007.

See www.StemCells.com for supporting information available online.